ORIGINAL ARTICLE

A COMBINED APPROACH ON HEAT TRANSFER ANALYSIS FOR LED BASED AUTOMOTIVE HEADLAMPS

| Moumouni Guero Mohamed [1,2,3*] | and | Prodjinonto Vincent [2,3] |

[1.] Dan Dicko Dankoulodo University of Maradi, UDDM | Republic of Niger |
[2.] Laboratory of Energetics and Applied Mechanics | University of Abomey Calavi | Republic of Benin |
[3.] Department of Mechanical and Energy Engineering | Polytechnic School of Abomey-Calavi | Republic of Benin |

| Received February 22, 2022 | | Accepted February 29, 2022 | | Published June 02, 2022 | | ID Article | Moumouni-Ref01-ajira220422 |

RESUME

Introduction: Les diodes électroluminescentes (DEL) composées d'InGaN et de phosphore jaune ont connu un développement très rapide au cours des dernières décennies grâce à leur haut rendement, leur chromaticité accordable, leur grande fiabilité et leurs avantages environnementaux. Bien que les LED présentent une efficacité de conversion énergétique très élevée, elles souffrent de nombreux problèmes dus à la température de jonction élevée (Tj). **Objectif** : notre objectif est d'étudier le transfert de chaleur pour les phares automobiles à LED. Une approche combinée avec la collecte de données expérimentales en utilisant une caméra infrarouge et un thermocouple pour mesurer la température sur la surface du phare, une analyse par éléments finis et une simulation numérique pour caractériser la distribution de chaleur sur le phare à LED est réalisée. En faisant varier la puissance d'entrée et la température ambiante, les effets correspondants sur la dissipation de chaleur sont observés et les points chauds sont ainsi détectés. **Résultats** : Enfin, une comparaison des résultats de la simulation numérique, de l'analyse par éléments finis et des données recueillies est effectuée pour vérifier la précision de l'étude. Les résultats ont montré un très bon accord avec moins de 5% d'erreur moyenne, ce qui valide la rigueur de cette étude. Cela montre que le modèle numérique peut être utilisé pour estimer les températures de surface en cas de conditions différentes dans un phare automobile.
***Mots-clés** : Phares à DEL pour automobiles ; imagerie thermique à haute résolution ; température de jonction ; simulations numériques, mesures thermiques.*

ABSTRACT

Background: Light Emitting Diodes (LEDs) composed of InGaN, and yellow phosphorus have undergone a very rapid development over the last decades with the high efficiency, tunable chromaticity, high reliability, and environmental benefit. Although LEDs boast exceedingly high energy conversion efficiency, they are suffering from many problems due to the high junction temperature (Tj). **Objective**: Our objective is to investigate the heat transfer for LED based automotive headlamps. A combined approach with experimental data collection by using an infrared camera and thermocouple to measure the temperature on the surface of the headlamp, finite element analysis, and numerical simulation to characterize the heat distribution on the LED headlamp is conducted. By varying the input power and the ambient temperature, the corresponding effects on the heat dissipation are observed and thus hot spots are detected. In the end, a comparison of the results of the numerical simulation, FEA, and the collected data is performed to verify the accuracy of the study. **Results:** The results showed particularly good agreement with less than 5% average error, which validates the strictness of that investigation. It shows that the numerical model can be used to estimate the surface temperatures in case of different conditions in an automotive headlamp.
***Keywords:** Automotive LED headlamps; high-resolution thermal imaging; Junction temperature; numerical simulations, thermal measurements.*

1. INTRODUCTION

Light-emitting diodes (LEDs) have become immensely popular as a future lighting system with the advantages of high efficiency, adjustable chromaticity, and excellent reliability. Despite LEDs were developed about 40 years ago, significant uses for various lighting applications have only been observed in the last 20 years. Current lighting technologies are apparently ineffective, and LEDs are seen as a promising technology for saving energy and reducing associated greenhouse gas emissions. D. Almeida and al., (2014) reviewed the potential and challenges of solid-state lighting (SSL) in Europe and projected that SSL will become a dominant effective light source by 2020 [1]. Current developments in LED technologies have resulted in various applications, including the use of LEDs in a car headlight for forward lighting. However, thermal management is one of the key issues, which requires attention to develop a stable LED operation and a long service life.

The chips currently used for lighting are available with input power ranging from 1 W to 25 W with an area less than 1 mm^2, corresponding to the heat flux of more than 100 W / cm^2 [2]. The main objective of a thermal management system of LED headlamps is to maintain the temperature of the LED junction and near the lowest possible for the stability, reliability, and longevity of LED. X. Long et al., (2015) and Raypah and al., (2018) reviewed the use of LED on a headlamp and conclude that LED headlamps experience a long period of sustained growth and are gaining in popularity due to the development of energy-efficient thermal management, adaptive driving beams, and functional controller ensure the markets and consumers really benefit from the LED headlamp [3, 7]. The thermal management of the LED lamp comprises two main factors: the packaging and the performance of the system [4]. Regarding the heat dissipation section, natural convection heat sinks are the most used for cooling the LED lamp because of its zero-

*Corresponding author Author & Copyright Author © 2022: | Moumouni Guero Mohamed * |.

energy consumption. Numerical and experimental studies have been developed. The effects of geometric parameters (such as length, height, and number of fins) and orientation of the packaging have been widely studied to optimize the design of the heat sink [5, 19]. Ben Abdelmlek and al., (2016) have studied the effect of the deficient conduction path between the heat sink and LED, and they have demonstrated that it largely affects the thermal behavior and photometric properties of the module [9]. In addition, numerical and analytical studies of the thermal resistance model [6, 10] and thermal spreading resistance were performed. It has been found that thermal spreading resistance may have a significant effect on the thermal behavior of the package. Kai-Shing Yang et al., (2014) and Shen Yingdong et al., (2021) conducted an experimental and numerical study of heat transfer in high-power LEDs [8, 11]. Their results indicate that the effect of thermal spreading resistance increases with the increase of the injected power. Yovanovich and al., (1999) obtained a solution for thermal spreading resistance of a centrally located heat source on a compound rectangular flux channel [12]. Their general solution can also be used to model any number of discrete heat sources on a compound or isotropic flux channel using superposition. Ben Abdelmlek and al., (2017) have developed a numerical study on thermal behavior of high-power LED et conclude that the higher hot spot on the module is located at the junction point of the chip [13]. Manoj Kumar and al., (2015) proposed a heat transfer analysis of an automotive headlamp by comparing CFD results and measured data [14]. Their CFD simulations on the models have shown a fair agreement with the experimental work by determining the same hot spot on the headlamp.
In this study, a numerical simulation, a series of experiments, especially thermal performance tests, and a finite elements analysis were performed to investigate the heat transfer characteristics of LED automotive headlamps. Finally, we discuss and compare the different values determined by the FEA, numerical simulation, and measured data to conclude about heat dissipation.

2. MATERIELS AND METHODES

2.1 Numerical method

In this section, we discuss numerical simulations. A numerical simulation may be a calculation conducted on a computer following a program implementing a mathematical model for a physical system. Numerical surface simulations are needed to verify the behavior of systems whose mathematical surface models are too complicated to produce analytical solutions, as in most nonlinear systems.

2.1.1 General analytical solution

a. Governing Equations and Boundary Conditions

The governing equation for the system shown in *Figure 2* is Laplace's equation: [12]

$$\boldsymbol{\nabla^2 T = \frac{\partial^2 T}{\partial x^2} + \frac{\partial^2 T}{\partial y^2} + \frac{\partial^2 T}{\partial z^2} = 0} \quad \textbf{(1)}$$

which is subjected to a uniform flux distribution:

$$\boldsymbol{\left.\frac{\partial T}{\partial z}\right|(z = 0) = -\frac{(\frac{Q}{As})}{K1}} \quad \textbf{(2)}$$

Within the heat source area, As = cd, and

$$\boldsymbol{\left.\frac{\partial T}{\partial z}\right|(z = 0) = 0} \quad \textbf{(3)}$$

Outside the heat source area and a convective or mixed boundary condition on the bottom surface

$$\boldsymbol{\left.\frac{\partial T}{\partial z}\right|(z = 0) = -\frac{h}{K1}[T(x, y, t1) - Tf]} \quad \textbf{(4)}$$

In extended surface applications such as heat sinks, the value of *h* replaced by an effective value, which accounts for both the heat transfer coefficient on the fin surface and the increased surface area [17].
Along the edges of the plate, the following conditions are also required:

$$\boldsymbol{\left.\frac{\partial T}{\partial x}\right|(x = 0, a) = 0}$$

And

$$\boldsymbol{\left.\frac{\partial T}{\partial y}\right|(y = 0, b) = 0}$$

The general solution for the total thermal resistance and temperature distribution obtained for the system shown above. The thermal resistance for the configuration shown in this case is a function of $R = f(a, b, c, d, Xc, Yc, t1, h, k1)$

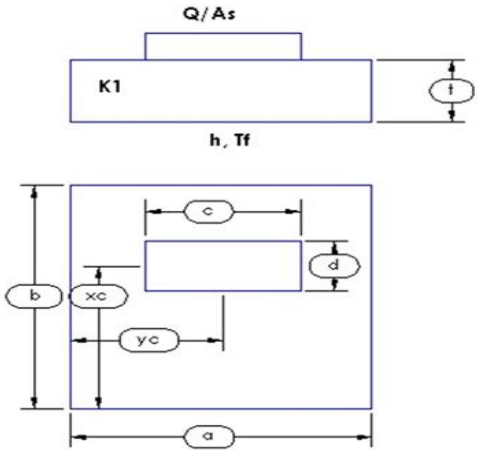

Figure 1: represents the baseplate and the chip with the characteristics and dimensions.

b. General Solution

The solution for the isotropic plate may be obtained by means of separation of variables. The solution is assumed to have the form u (*x,y,z*) = *X*(*x*)* *Y*(*y*)**Z*(*z*), where u (*x,y,z*) = *T*(*x,y,z*) - *Tf* . Applying the strategy of separation of variables yields the subsequent general resolution for the temperature excess within the plate that satisfies the thermal boundary conditions (*x*=0, *x*=*a*) and (*y*=0, *y*=*b*)

$$\theta(x,y,z) = Ao + Bo + \sum_{m=1}^{\infty} \cos(\lambda x)\,[A1\cosh(\lambda z) + B1\sinh(\lambda z)] + \sum_{n=1}^{\infty} \cos(\delta y)\,[A2\cosh(\delta z) + B2\sinh(\delta z)] + \sum_{m=1}^{\infty}\sum_{n=1}^{\infty} \cos(\lambda x)\cos(\delta y)[A3\cosh(\beta z) + B3\sinh(\beta z)] \quad (5)$$

Where $\boldsymbol{\lambda} = m\pi/a$, $\boldsymbol{\delta} = n\pi/b$, and $\boldsymbol{\beta} = \sqrt{(\lambda^2 + \delta^2)}$.
The solution contains four components, a uniform flow solution and three spreading (or constriction) solutions which vanish when the heat flux is distributed uniformly over the entire surface z=0. Since the solution is a linear superposition of each component, they may be dealt with separately. Application of the boundary conditions in the z-direction will yield solutions for the unknown constants.
Application of the thermal boundary condition at z=t_1 for anisotropic rectangular plate yields the following result for the Fourier coefficients:

$$\boldsymbol{Bi} = -\boldsymbol{\Phi}(\zeta)\boldsymbol{Ai} \qquad \boldsymbol{i} = 1,2,3$$

where

$$\boldsymbol{\Phi}(\zeta) = \frac{\zeta\sinh(\zeta t1) + \frac{h}{K1}Cosh(\zeta t1)}{\zeta\cosh(\zeta t1) + \frac{h}{t1}\sinh(\zeta t1)} \quad (6)$$

and ζ is replaced by $\boldsymbol{\lambda}$, $\boldsymbol{\delta}$, or $\boldsymbol{\beta}$, accordingly.
In our case, the dimensions of a plate or circuit board are a=20 mm, b=20 mm, t1=2 mm, t2=1mm, h=170 W/m2K and k1 = 400 W/mK, K2 = 130, with Tf=25°C. The heat source having dimensions c=4 mm and d= 0.4 mm. The source with a power in range of Q = 0.6825 to 3.5 W is located at Xc = 10 mm and Yc = 15 mm. The basic equations programmed into any symbolic or numerical mathematics software package. For the present calculations, MATLAB application is used, employing 50 terms in each of the single and double summations.
The figure below shows a simplified model for numerical simulations.

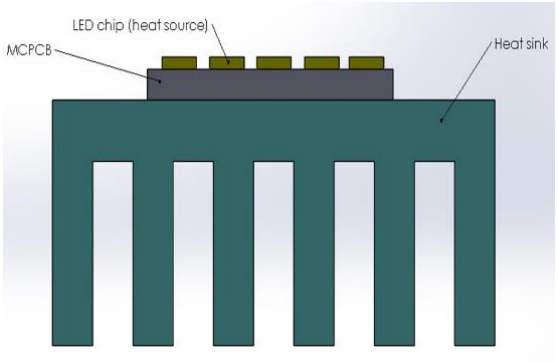

Figure 2: Configuration of LED modules for numerical simulations.

2.2 Experimental analysis of headlamp

2.2.1 Test sample description

Experimental analysis carried out on an automotive headlamp to establish the thermal characteristics and behavior. The high-power LED packaging for our headlamp application is LUMILEDS LUXEON Altilon H1K PnP. High-power automotive forward lighting LED - LUXEON Altilon LEDs deliver distinctive brilliant white light for forward automotive lighting design while delivering the efficiency that leaves a power to spare for other accessories. This type of LED chip can work in the temperature ranges -40 to 150°C, the maximum permissible junction temperature is 130°C, the light-emitting area is less than 1 mm², and the typical CCT is 5600K, its colorimetric properties conform to the ECE regulation. For the photoelectric parameters, see *Table 1* [15]. F*igure 3* presents a solid modeling of the headlamp and the led module used in this study.

Table 1: Photoelectric parameters of the chip.

Parameters	Min	typical	Max
Current (mA)	100	700	1500
Voltage (V)	13.90	16	17
Thermal Resistance (K/W)		1.1	1.5

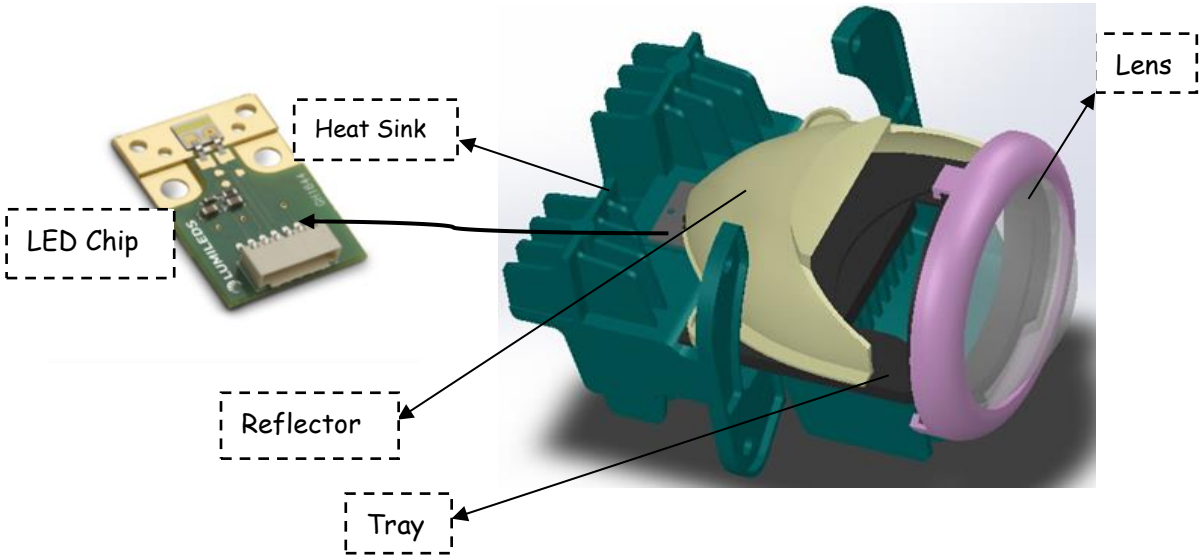

Figure 3: Solid model and LED module used on the headlamp.

2.2.2 Thermal measurements

Two (2) measurement techniques are used to characterize the temperature distribution of the LED package for the operating power in a temperature-controlled environment (T_{air} = 25°C). One method consists of measuring the temperature using thermocouples placed on four locations (the heat sink, tray, lens and on the chip). The other approach is using a high-resolution thermal imaging camera to characterize the heat distribution over the surface and estimate the LED junction temperature. The LED module mounted on the aluminum heat sink placed horizontally in a temperature-controlled environment and allowed to be cooled by natural convection. The thermal imaging camera placed directly above the package to get a top view of the system. Figure 4 shows the measurement setup and the thermal image of the system. The thermal imager used was the Fluke Thermal Imager Ti55, which has a high resolution and the accuracy of ± 0.1% of the reading + 0.5 ^{O}C on non-reflective surfaces. The forward voltage and current measured with the help of digital clamp multimeters. It observed that there is a constant supply of power to the chip, and it calculated to be 1 W. The same used for achievement the FEA simulation on the headlamp by fixing a constant flux condition on the lamp surface. After connecting all the necessary equipment, the headlamp switched on. The headlamp reached a steady state condition within a half of an hour and then, the temperature readings are taken. *Table 2* presents the equipment used in data collection and its parameters. From the IR (InfraRed) image, it was clear that the high-temperature region obtained on the top side of the LED module surface. The measurement results discussed in more detail and compared to the results of the simulations in discussion.

Table 2: Instruments accuracy.

Instrument name	Measured property	Accuracy of the instrument
DT – 830B multimeter	Current	± 0.5% 5D
	Voltage	± 2% 5D
Fluke Thermal Imager Ti55	Temperature	± 0.1% of the reading + 0.5 ^{O}C
JINKO HAND-WELD Meters	Temperature	± 0.1% +1°C

a)

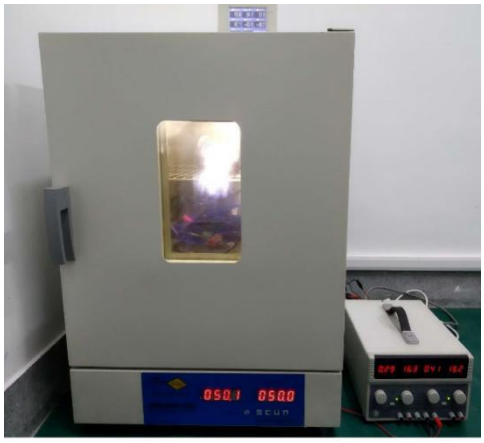

b)

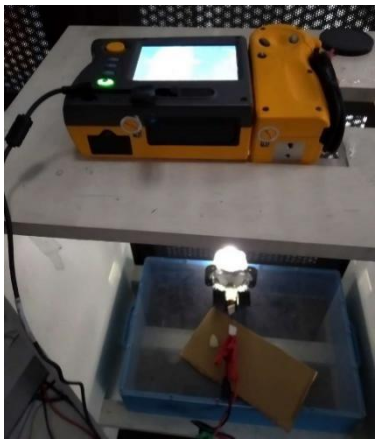

c)

Figure 4: Measurement and experimental setup: **a**) thermocouple; **b**) Heat Box; **c**) Infrared camera.

2.3 Finite Element Analysis simulation

In this section, the boundary conditions, geometry, and mesh created to perform the finite element analysis of automotive headlamps are discussed. The results obtained based on the experiment conducted will be presented later in this section.

Boundary Condition

The material specifications and constants used for the analysis are set. The computational domain divided into fine control volume. In this study, a LED Chip (describe in section 1.1) was used, which is supplied with a power of 1W as measured with the help of digital clamp multimeters. On all the exposed surfaces of the headlamp, a heat flux prescribed that allows for convective heat transfer to the surroundings. Thermal radiation ignored for the polished surfaces since the surface emissivity coefficient is about 0.05.
The heat transfer coefficient *h* depends on the surface orientation and temperature. The heat transfer coefficient of a surface in ambient air estimated by [13, 18]:

$$hc,i = C\left(\frac{\Delta T(x,y)}{Lfin}\right)^n = C\left(\frac{Ts(x,y)-T0}{Lfin}\right)^n \quad (7)$$

where *Ts(x,y)* is the surface temperature on location *(x,y)* and T_0 is the ambient temperature. *Table 3* shows the constants and exponents for the calculation of the heat transfer coefficient for different surface orientations. The length of the fin defined by *Lfin*.

Table 3: The values of constant C and exponent n for different surface orientations

Plate orientation	C	n
Vertical	0.7	0.25
Horizontal (Top-side)	0.7	0.25
Horizontal (Bottom-side)	0.3	0.25

The internal heat calculated by the formula:

$$Pi = \frac{P * \mu led}{V} \quad (8)$$

Table 4: Material parameters of each layer [16].

Layer	**Material**	**Thermal conductivity (W m-1 K-1)**
Heat sink	Al	237
PCB board	PCB	178
Glue line	Sn-Pn metal	68
Alumina substrate	Al2O3	10
GaN	GaN	30
Epoxy lens	Epoxy	0.8
Reflector	PBT (Glass reinforced)	0.27
Shell	PBT (Glass reinforced)	0.27

Table 5: Tests conditions for different simulations cases and experiments.

Items	**Specifications**						
Ambient Temperature (°C)	10	20	30	40	50	60	70
Input Current (mA)	100	200	300	400	500	600	700
Power (W)	0.45	0.6825	1	1.6	2	2.8	3.5
Time (s)	1800						

3. RESULTS

To avoid measurement errors and increase the reliability of the comparisons, different measurement conditions are tested, acting on the current and therefore the power of the lamp. The experimental conditions are the same in both cases. The variation of the current is If = 100 ~ 700 mA. Here are the results of different simulations done.

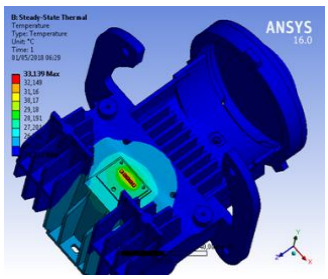

FEA Simulation (200 mA)

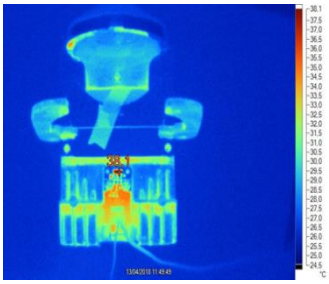
Experiment result (200 mA)

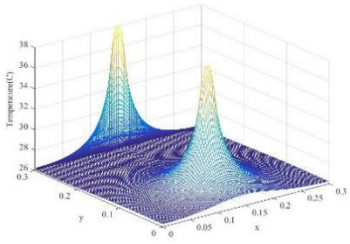
Matlab simulation (200 mA)

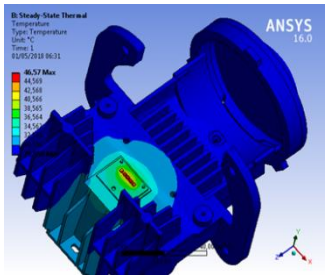

FEA Simulation (350 mA)

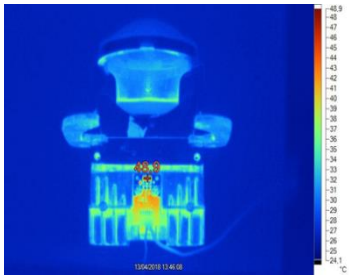
Experiment result (350 mA)

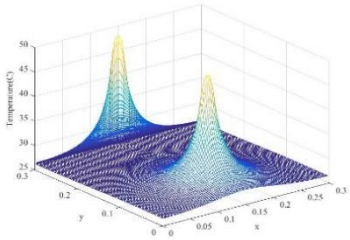
Matlab simulation (350 mA)

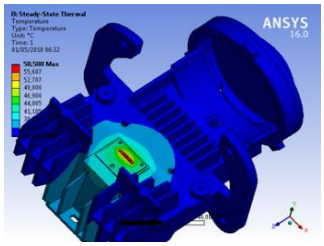

FEA Simulation (500 mA)

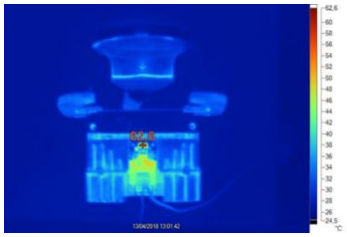
Experiment result (500 mA)

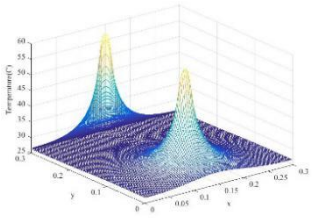
Matlab simulation (500 mA)

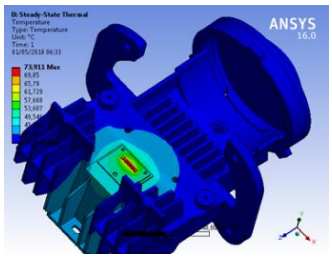

FEA Simulation (600 mA)

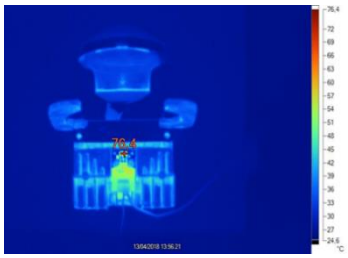
Experiment result (600 mA)

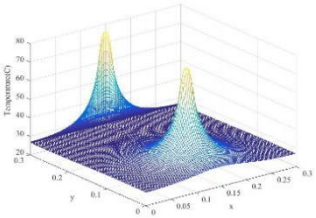
Matlab simulation (600 mA)

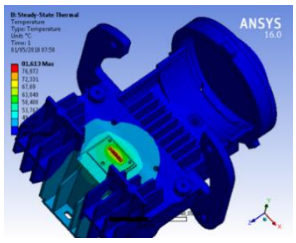

FEA Simulation (700 mA)

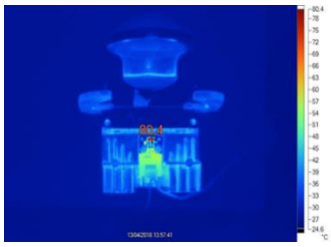
Experiment result (700 mA)

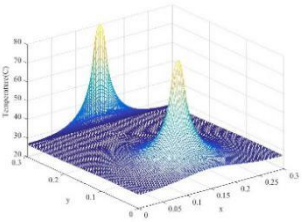
Matlab simulation (700 mA)

The following table summarizes the results obtained during simulations and measurements by using IR camera, thermocouples, finite element analysis and numerical simulations in seven different conditions.

Table 6: Results for the study (°C).

Power	Temp. FEA	Temp. Experiments		Temp. Simulation
		IR Camera	Thermocouple	
0.45	28.5	28	31	29
0.6825	35.8	38.1	39.1	35.5
1	40	42.3	42.8	41.6
1.6	48.3	48.9	50.2	48.7
2	57.375	62.6	63.4	59
2.8	71.7	76.4	77.1	73
3.5	80.7	80.4	81.8	80

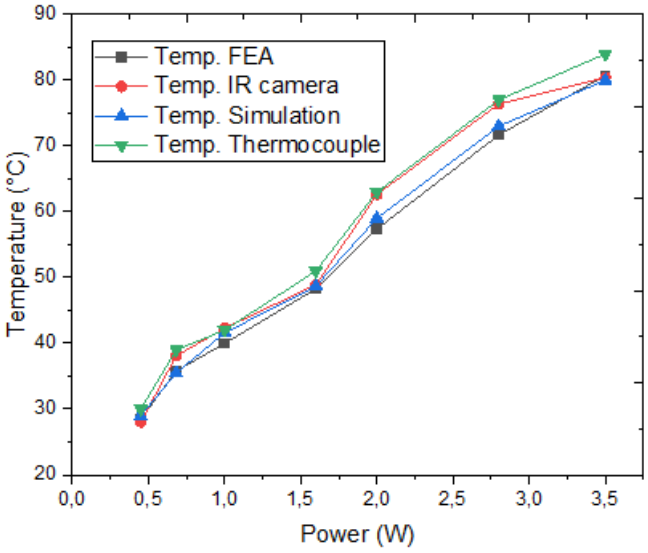

Figure 5: Comparison of the results from simulations and measurements in different operating conditions.

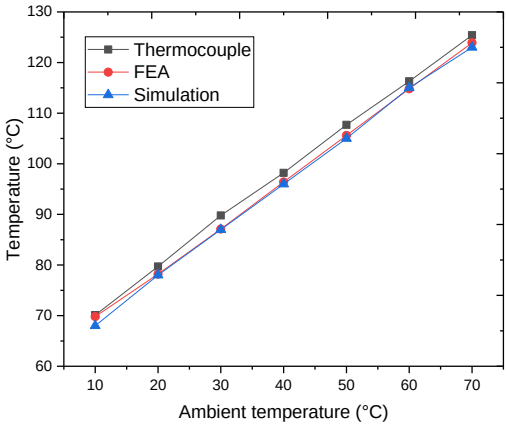

Figure 6: Junction temperature changes vs. the ambient temperature on condition 7 (700 mA) numerical

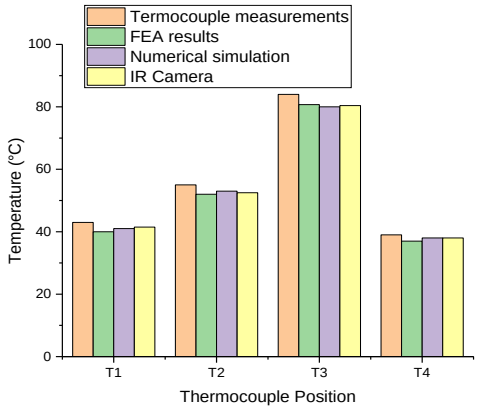

Figure 7: Comparison of the temperatures between measurement by the thermocouple, IR camera, simulation and FEA result on condition 7 on different headlamp locations

4. DISCUSSION

The comparison between the simulation and the measurements of the IR camera and thermocouple is shown in Figure 5. There is a good agreement between the model and the measurement. The differences can be explained by Joule heating interconnects that were not accounted for in the model. Furthermore, the IR temperature measurement is influenced by the different emissivity coefficients of the materials of the package and heat sink material.

Most of the car headlamps are installed in the engine compartment, so it can use limited space. Otherwise, headlamps are too close to the water tank, engine, air conditioning; its working temperature can be as high as 70°C [20]. Figure 6 shows the effect of ambient temperature changes at the junction temperature. In this study, experiment data was collected through thermocouple and obtained results by FEA and numerical simulations by

changing the ambient temperature during the simulation.

For the measurement with the thermocouple, four (4) locations selected to collect a good dissipation of the temperature. The locations are the heat sink (T4), tray (T2), lens (T1) and on the chip (T3). Therefore, data were collected to compare with the simulation results. All the test conditions are the same as in the previous cases. *Figure 6* shows that the measurements of the thermocouple are in good agreement with the numerical and FEA simulations. The package appears to heat up at a higher rate than the model predicts. It is assumed that Joule heating of the wire interconnects can explain this.

Figure 7 shows the comparison of the temperature distribution obtained through IR camera and thermocouple measurements, FEA, and numerical simulation results. From the temperature profile pattern for the IR images, thermocouple, FEA, and the numerical simulation that the location of the high-temperature region is exactly matching, and it is on the chip. The magnitude of temperature obtained through numerical simulations can be clearly validated with the testing and FEA results.

It can be observed that regions susceptible to thermal degradation may be the chip due to the high heat concentration. Thus, we should take caution when designing the geometry of the headlamps and appropriate heat transfer analysis should be performed to detect the risks at the beginning of the design phase.

5. CONCLUSION

This investigation shows a comparison between an experiment, FEA, and a numerical simulation of heat dissipation on a LED automotive headlamp under different boundary conditions. Experiments by collecting data using IR camera and thermocouples are conducted under different conditions and by changing the ambient temperature in order to subject the headlamp to the same conditions as in the automotive using conditions. After experiment data collection, finite element analysis, and numerical simulations to determine the heat distribution was performed and determined the hot spots on the headlamp during operation.

A comparison of results obtained from the four methods allows us to validate the study.
Based on the foregoing discussions, the following conclusions can be drawn:

- There is a certain deviation between the test results, the FEA, and the numerical simulation results, and the deviation increases with the ambient temperature or input power rising, but the maximum deviation is lower than 5%, within the acceptable range. It indicates that the method of numerical simulation is feasible.
- The highest temperature point on the chip changes linearly with the ambient temperature or input power.
- Some conditions were simplified in the simulation and the LED headlamp used in the experiment is a modified lamp, it did not consider the change in optical performance in the thermal design. Thus, further research may be considered for a better estimate of heat dissipation.

Futures works will focus on the optimization of the headlamp with the aim of offering the best possible heat sink. For that, several solutions are possible. We can act on the shape of the heat sink, the choice of its material or finally act on the arrangement of the LEDs on the chip.

Nomenclature

SSL = Solid State Lighting
LED = Light Emitting Diode
Tj = Junction temperature °C
Pi = internal heat W/m^3
Lfin = length of the fin, m
V= Volume m^3
a, b, c, d = linear dimensions, m
A_b = baseplate area, m^2
As = heat source area, m^2
A0, Am, An, Amn = Fourier coefficients
Bi = Biot no., hL/k
Cp = heat capacity, J/Kg. K
h = contact conductance or film coefficients, W/m^2. K
i = index denoting layers 1 and 2
m, n = indices for summations
IR: InfraRed
q = heat flux, W/m^2
k, k1, k2 = thermal conductivity, W/m. K
Q = heat flow rate, W
N = no. of heat sources
Xc, Yc = heat source centroid, m
Tf = sink temperature, K
T1, T2 = layer temperatures, K
t, t1, t2 = total and layer thicknesses, m
ζ , $\boldsymbol{\lambda}$, $\boldsymbol{\beta}$, $\boldsymbol{\delta}$ = eigenvalues

Acknowledgments: The work described in this paper was partially supported by the University Dan Dicko Dan Koulodo of Maradi, Republic of Niger and the Laboratory of Energetics and Applied Mechanics of the University of Abomey Calavi, Republic of Benin. May they find our sincere thanks.

Author Contributions: Moumouni Guero Mohamed conceived, designed, and performed the experiments; Moumouni Guero Mohamed analyzed the data; PRODJINONTO Vincent contributed reagents/materials/analysis tools.

Moumouni Guero Mohamed authored the paper.

Conflicts of Interest: The authors declare no conflicts of interest. The sponsors had no role in the design of the study; analyses or interpretation of data; in the writing of the manuscript, and in the decision to publish the results.

6. REFERENCES

1. Almeida D, Santos B, Paolo B, Quincheron M. Solid State lighting review – Potential and challenges in Europe. Renew. *Sustainable Energy. Rev. 2014;* 34: 30 – 48

2. Yung K C, Choy H S, Cai Z X. Thermal investigation of a high brightness Led array package assembly for various placement algorithms. *Applied Thermal Engineering*. 2014; 63: 105 – 118.

3. Long X, He J, Jing Z, Liang F, Xia Z and al. A review on light-emitting diode based automotive headlamps. *Renewable and Sustainable Energy Reviews*. 2015; 41: 29–41

4. Shyu J, Hsu K, Yang K, Wang C. Thermal characterization of shrouded plate fin array on an LED backlight panel. *Applied Thermal Engineering*. 2011; 31: 2909-2915.

5. Vítor A F C, António M G. Improved radial heat sink for led lamp cooling. *Applied Thermal Engineering.* 2014;70: 131-138. Available on: https://doi.org/10.1016/j.applthermaleng.2014.04.068

6. Sümer Y, Karaman O, Karaman C. Design and Thermal Analysis of High Power LED Light. European Mechanical Science. 2021; 5(1): 28-33.

7. Muna E R, Dheepan M K, Mutharasu D, Shanmugan S, Fauziah S. Variation of thermal resistance with input current and ambient temperature in low-power SMD LED. *Microelectronics International*. 2018; 35(1):1-11. Available on: https://doi.org/10.1108/MI-08-2016-0055

8. Yingdong S, Junfeng D, Yanlong W. Numerical Analysis of Thermal Management for High Power LED Array. E3S Web of Conferences 257, 01033 (2021). **DOI:** 10.1051/e3sconf/202125701033

9. Ben Abdelmlek K, Araoud Z, Ghnay R, Abderrazak K, Charrada K, Zissis G. Effect of thermal conduction path deficiency on thermal properties of LEDs package. *Applied Thermal Engineering*. 2016;102: 251–260.

10. Christensen A., Graham S. Thermal effects in packaging high power light emitting diode arrays. Applied Thermal Engineering. 2009;29: 364-371.

11. Kai-Shing Y, Chi-Hung C, Cheng-Wei T, Cheng-Chou W, Tsung-Yi Y, Ming-Tsang L. Thermal spreading resistance characteristics of a high-power light emitting diode module. *Applied Thermal Engineering*. 2014;70:361-368. https://doi.org/10.1016/j.applthermaleng.2014.05.028

12. Yovanovich M M, Muzychka Y S, Culham J R. Spreading Resistance of Isoflux Rectangles and Strips on Compound Flux Channels. *J. Thermophys. Heat Transfer*. 1999;13: 495–500.

13. Ben Abdelmlek K, Araoud Z, Charrada K, Zissis G. Optimization of the thermal distribution of multi-chip LED package. *Applied Thermal Engineering*. November 2017;126(5):653-660. **DOI**: https://doi.org/10.1016/j.applthermaleng.2017.07.136

14. Manoj K, Kumar N S, Raj R. Heat Transfer Analysis of Automotive Headlamp Using CFD Methodology. International Journal of Innovative Research in Advanced Engineering (IJIRAE) ISSN: 2349-2163 Issue 7, Vol 2.

15. LUXEON Altilon H1K PnP: Integrated functionality for headlight solutions. PB131 LUXEON Altilon H1K PnP Product Brief ©2017 Lumileds Holding B.V. Available on: https://www.lumileds.cn.com/wp-content/uploads/files/PB131.pdf

16. Thermal Management of XLamp® LEDs: APPLICATION NOTE. Available on: https://cree-led.com/media/documents/XLampThermalManagement.pdf

17. Muzychka Y S, Culham J R, Yovanovich M M. Thermal Spreading Resistance of Eccentric Heat Sources on Rectangular Flux Channels. *J. Electron. Packag*. Jun 2003;125(2):178-185. DOI: https://doi.org/10.1115/1.1568125

18. Xin-Jie Z., Yi-Xi C., Jing W., Xiao-Hua Li, Chun Z. Thermal model design and analysis of the high-power LED automotive headlight cooling device. *Applied Thermal Engineering*. 2014;1–11.

19. Wang J, Yi-xi C, Xin-jie Z, Chun Z. Thermal design and simulation of automotive headlamps using white LEDs. *Microelectronics Journal*. February 2014;45(2): 249-255. Available on: https://doi.org/10.1016/j.mejo.2013.11.011

20. Guzej M, Horsky J. Experimental Verifications and Numerical Thermal Simulations of Automobile Lamps. 2016;50(3):289. DOI: 10.17222/mit.2014.149

Cite this article: Moumouni Guero Mohamed, and Prodjinonto Vincent. A COMBINED APPROACH ON HEAT TRANSFER ANALYSIS FOR LED BASED AUTOMOTIVE HEADLAMPS. *Am. J. innov. res. appl. sci. 2022; 14(6): 272-280.*